Assessment of aquaporins function in stages of liver fibrosis using multi-b diffusion weighted magnetic resonance imaging

LI Qiu-ju[1], ZHANG Zi-heng[2], LI Jia-hui[1], YU Bing[1], ZHANG Xin[1], ZHAO Zhou-she[2], SHI Yu[1], XIN Jun[1], and GUO Qi-yong[1]

[1]*Radiology, Shengjing Hospital of China Medical University, Shenyang, Liaoning, China,* [2]*General Electronic Company Healthcare (China), Beijing, China*

Introduction: Liver fibrosis, an abnormal proliferation and deposition of connective tissue in liver induced by chronic liver diseases, could be reversible in a certain circumstance, while turns into irreversible if the causes persist with a gradual worsening[1]. Diffusion weighted (DW) MRI techniques, based on the Brownian motions of water molecules between tissues and cells, is considered an effective, molecular level evaluation method of liver fibrosis[2]. Since the introduction of intra-voxel incoherent motion (IVIM), DW MRI that performs a multiple b-value (multi-b) acquisition has been prevalent and gradually dominated the examinations of liver fibrosis with enriched information explored through the application of a non-monoexponential mathematic model[3], e.g. bi-exponential model[3], stretched exponential model[4], etc., which all provide certain biomarkers to improve clinical diagnosis in both precision and specificity. However, the discovery of the aquaporin family of water channels by Agre in 1993 brought a novel understanding of the transport mechanism of water molecules across cell membranes[5]. And it has been getting clear that the physiological functions of aquaporins are substantially involved in multiple different illnesses including abnormality of kidney function, loss of vision, brain edema, and liver fibrosis as well[6]. Thus, it is important to clearly understand the state variation of the corresponding AQPs in a fibrotic liver. In this study, we investigated the variation of apparent diffusion coefficients (ADCs) resulted from a DW MRI measurement before and after the administration of AQP1, AQP3 and AQP4 inhibitor, acetazolamide, which blocks the pathways for water molecule transportation, to seek the relationship between the ADC values and the correspondent of AQP expression. In addition, the histopathological and immunohistochemical tests were also executed in vitro to obtain the AQP expression and distribution on the hepatic tissue at different fibrotic stages as the "gold standard" for reference. Combining both, one can get, at a molecular imaging level, the relationship between the ADCs at high b values and the staging of liver fibrosis, so as to reach the purpose of this study, to realize early diagnosis of liver fibrosis and fibrotic stage evaluation using multi-b DW MRI techniques.

Materials and Methods:

1. Rodent liver fibrosis model preparation: 30 male Wistar rats was randomly divided into two groups, one model group with 24 and one control group with 6. For the model group, thioacetamide (TAA, Sigma/Aldrich, US) was intraperitoneally injected thrice a week, respectively on Monday, Wednesday and Friday, at a dose of 300 mg/kg on body weight. 4 model rats and 1 baseline rat were preformed MRI scan respectively after one-, two- , three-, four-, five-week modeling, and five-week modeling followed by one-week spontaneous recovery.

2. MR scanning: The rats were fast and dehydrated for 6 hours before MR scanning and anesthetized right before the measurement. The MR data were collected using a 5 cm diameter animal coil (Chenguang Corp., China) with the rats positioned in prone at a 3.0 T scanner (GE HDxT, Mikauwee). Besides the conventional T1WI and T2WI performed, a multi-b DWI was carried out with 18 b values selected from 0 to 4500 s/mm^2. Scan parameters were as following: TR/TE 5.43/1.56ms, flip angle 30°, FOV 150*150mm², spatial resolution: 0.59*0.59mm², slice thickness 5.0 mm. Afterwards, both the model and baseline rats were injected 1 ml acetazolamide solution with a mass concentration of 1mg/ml through the caudal vein to inhibit the AQP1, AQP3 and AQP4 on hepatic tissue. The MR measurements were then performed again with the same imaging parameters.

3. Image post-processing: A newly developed tri-exponential model equipped at an Advantage Workstation (GE, Mikauwee) was applied for the DW images post-processing. Empirically, the thresholds that separated the low-b, middle-b and high-b domains were defined as 200 s/mm^2 and 1700 s/mm^2. Two regions of interest (ROIs), was selected respectively on left- and right- lobes with an attention of avoiding the large blood vessels in liver, bile duct and artifacts, and then projected onto the four obtained color-coded mappings, standard ADC, low-b ADC, middle-b ADC and high-b ADC, for statistical analysis, Fig. 1.

4. Pathology analysis: A central-slice of each liver lobe, basically the same layer as the sampling slice for DWI analysis, was chosen for the routine HE staining, Sirius red staining of collagen and AQP1 molecular pathology staining to determine the stage of liver fibrosis and the AQP1 expression level, Fig.2. Liver fibrotic stage was analyzed by Mevatir criteria.

5. Statistical analysis: SPSS17.0 software was applied for statistical analysis, with $p<0.05$ considered statistically significant.

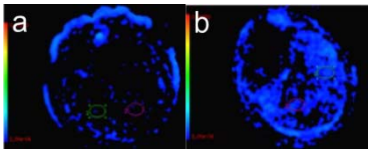

Fig. 1 ADC mappings of a control (a) and a S1model rats (b) fitted at high b values from the tri-exponential model.

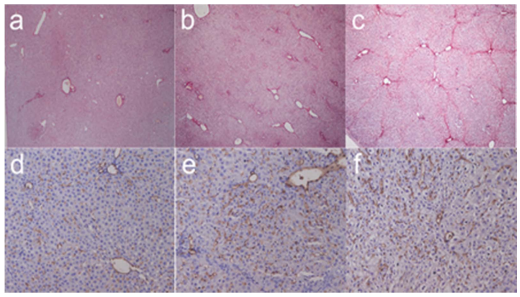

Fig.2 Histopathological (Sirius red staining, a-c) and immunehistochemical (AQP1 molecular pathology staining, d-f) photos of hepatic tissues at healthy, S1 and S2 liver fibrosis.

Results: The AQP1 expression in the liver endothelial cells significantly increased with aggravation of liver fibrosis from normal to cirrhosis, Fig. 2, with the overexpression usually located at new fiber spacing mainly in vascular endothelial cells. As shown in Tab.1, an obvious increase of perfusion was observe at S1 but a significant decrease (>50%) occurred with the addition of inhibitor. At S2, perfusion decreased, and further decreased (>20%) with inhibitor. AQP expression further increased vs. S1. The inhibition tests were all negative.

Tab. 1 The ADC values ($\times 10^{-3}$mm^2/s) pre and post inhibitor injection from mono- (std.) and tri-exponential models (low-b, mid-b and high-b), corresponding inhibition rate was computed

ADC	Pre Inhibitor Projection				Post Inhibitor Projection				Inhibition Rate			
	Std.	Low-b	Mid-b	High-b	Std.	Low-b	Mid-b	High-b	Std.	Low-b	Mid-b	High-b
Control	4.90	47.8	4.7	0.5	5.2	42	8.03	0.45	-6.1%	12.13%	-70.8%	10.00%
Model S1	5.0	52.9	6.5	0.9	4.6	24	5.0	0.9	8.00%	54.63%	23.08%	0.00%
Model S2	5.37	30	7.85	0.75	5.79	23.2	8.0	1.6	-7.8%	22.67%	-1.9%	-106%

Discussion: 1. An obvious signal difference between the experimental group and the control group was observed. 2. DW MRI at low-b value reflected the hepatic blood perfusion, while functional changes of the AQPs on cell membranes at high b-value. At an early stage of liver fibrosis, a more severe fibrosis corresponds to a higher compensatory AQP expression occurred. 3. Acetazolamide could efficiently suppress the membrane AQP function. 4. Limitations of the study: (1) On liver cell membranes, AQP3, AQP8, AQP9, AQP11 are all richly distributed. Thus, acetazolamide, merely effective to AQP1, AQP3 and AQP4 was lack of specificity for an entire AQP inhibition. In addition, not only water molecules but urea, glycerol and nitrite all transport through AQPs. Therefore, a further study of the function and specificity of AQPs is required. (2) TAA can induce a more stable liver fibrosis modeling than CCl_4. However, due to the individual differences on weight of the rats, it is hard to control the right time of modeling for a desired fibrotic stage.

Conclusion: In summary, it was demonstrated in this study (1) the severity of liver fibrosis is positively correlated with the AQP1 expression and (2) the multi-b DW MRI technique was capable to detect the S1 stage liver fibrosis, thus a promising tool to realize an early diagnosis of liver fibrosis.

References: 1. Bataller R, DA BrennerJ Clin Invest. 2005;115(2):209–218; 2. Annet L, et al., JMRI 2007;25:122–128. 3 April MC, et al., JMRI 2012;36:159–167; 4. Nina T, et al, ISMRM 2012, 4112; 5. Agre P, et al., Am. J. Physiol. Renal Physiol.1993; 6. Agre P, David K, FEBS Letters 555 (2003) 72-78.